3D-Printed On-Fiber Fabry-Pérot Resonator for Refractive Index Measurements

Joanna Korec-Kosturek, [1,2] Monika Halendy, [1] Sławomir Ertman, [1] Konrad Osak, [1] Konrad Pogorzelec, [1] Piotr Lesiak*[1]

[1]*Faculty of Physics, Warsaw University of Technology, Koszykowa 75, 00-662 Warszawa,*
[2]*Military University of Technology, Faculty of Advanced Technologies and Chemistry, gen. Kaliskiego 2 St., 00- 908 Warsaw, Poland*

Received December 05, 2025; accepted December 30, 2025; published December 31, 2025

Abstract—In this paper, we present the results of measurements performed using a Fabry Pérot resonator printed on a fiber optic tip. Thanks to its design, the resonator allows for simple sputtering of both resonator mirrors with varying degrees of reflection in a single process step. Applying different reflectances to both resonator mirrors significantly increases the refractive index measurement range while maintaining excellent signal modulation (15 dBm for a refractive index of 1.477). Furthermore, our sensor features a wide measurement range (1350–1700 nm).

Recently, sensors based on optical fibers have been gaining popularity, which is understandable given that they can meet current requirements such as high-speed detection, high sensitivity, immunity to electromagnetic interference, corrosion resistance, and low production costs [1, 2]. Moreover, due to the development of micro- and nanotechnology, optical fiber sensors can be miniaturized and adapted to work in harsh environments where electrical sensors may fail [3, 4].

One of the simplest optical fiber sensors is based on the Fabry-Pérot (FP) interferometer [5–7]. Even with these simple sensors, maximum simplicity of solutions is promoted while maximizing sensitivity or application diversity [8]. Therefore, in this paper, we present research on optical fiber-based FP resonators printed as fiber tips. As a reference, we used tests performed with two optical fibers, utilizing both flat mirrors. Fiber tips were fabricated using two-photon polymerization (2PP) technology [9]. Significant emphasis was placed on creating a compact structure with a high-reflection mirror formed on the printed tip [10]. The concept of printing an optical cavity sensor onto an optical fiber tip was described in [11] and [12]. In these works, the signal is reflected from both the inner and outer surfaces of the printed mirror, so the sensor's response to changes in the refractive index results from the overlapping shifts of these two modulations. This is an interesting proposal; however, the solution presented there does not include sputtered mirrors.

* e-mail: piotr.lesiak@pw.edu.pl

To enhance reflection, we employed the cathode sputtering method to deposit thin metal films of varying thicknesses onto the printed surfaces. It is essential to note that the chosen manufacturing method is efficient, enabling the simultaneous control of several parameters of the fabricated FP resonator, including cavity length and the extent of metal layer coverage. This study builds upon our previous research and incorporates the conclusions from both our previous publications.

A Fabry-Pérot resonator is a typical multi-beam interferometric device. Figure 1 presents a schematic of the FP fiber-based sensor. Light passing through the fiber core is partially reflected at the end of the optical fiber, which is simultaneously the front face of the cavity due to Fresnel reflection at the silica/air interface (M_1). This first reflection is referred to as the reference signal, while the rest of the light beam is transmitted forward through the cavity. The second reflection occurs at the air/fiber interface (M_2) and generates the detection signal. The reference and detection signals can interfere with each other. Depending on the difference in optical path length between them, this interference can be either constructive or destructive, resulting in an interference signal [13]. The output intensity (I) of the reflected light beam can be written as [13]:

$$I = I_1 + I_2 + 2\sqrt{I_1 I_2}\cos\phi \quad (1)$$

where I_1 and I_2 are the beam intensities for the back-reflected reference and detecting signal, respectively, and ϕ represents the total phase difference between these components. The phase difference is related to the cavity length, and any change in the optical path length causes a change in the phase shift and is given by [13]:

$$\phi = \frac{4\pi n L_{cav}}{\lambda} \quad (2)$$

where n is the refractive index of cavity, L_{cav} is the length over which the phase change occurs, and λ is the laser

diode center wavelength. When constructing a sensor based on resonance phenomena, it is desirable to obtain a high resonance enhancement, resulting in resonance dips of high finesse and a high extinction ratio (the ratio between the optical power levels corresponding to the maxima and minima in the resonant spectrum), which enable the most precise measurements. Finesse is typically described as follows [14]:

$$F = \frac{FSR}{FWHM} \tag{3}$$

where Free Spectral Range:

$$FSR = \lambda^2/(2nL_{cav}) \tag{4}$$

corresponds to the spectral distance between two adjacent resonance dips, and FWHM (Full Width at Half Maximum) is the width of a resonance dip.

When considering a 3D-printed fiber-tip FP resonator, the output interference signal can be described using the three-beam interference model. The light beam is not only reflected at the silica/air and air-resin interfaces at the end of the cavity but is also reflected from both surfaces of the 3D-printed diaphragm. Therefore, the output interference signal involves three-beam interference. This leads to a phenomenon known as the Vernier effect [15]. This creates a complex interference pattern with a new, significantly greater periodicity compared to the FSR of the individual cavities. This effect is typically used to increase the sensitivity of measurements such as the refractive index [16], but despite its observation, we will not address it in our measurements.

To select the appropriate thickness of the gold layer sputtered on the FP resonator, we used standard single-mode fibers with pigtails having a core diameter of 8.2µm and a cladding diameter of 125µm. The quality of the cleave was monitored each time using a reflection loss measurement with a KINGFISHER KI7343C-INGAAS meter. The printed tips were placed in a low-vacuum Leica ACE200 sputter coater, with a vertical orientation towards the golden target. Sputtering is carried out at room temperature using an ionized working gas (Argon) under low-vacuum conditions of 10^{-2} mbar, with a current of 30 mA applied to the target. The layer thickness is measured with the quartz crystal microbalance.

The FP resonators, as fiber optic tips, were manufactured in two configurations: unshielded and shielded. In both cases, one of the reflective surfaces is the optical fiber end face, and the other is a roof printed on the supports, as shown in Fig. 1. The selected cavity length in each considered case was L_{cav} = 50µm. The outer diameter of the proposed structure was 80µm, and the thickness of the flat reflective surface was 5µm. In one case (unshielded tip), the supports were spaced as straight columns. In the other case (shielded tip), the supports consisted of three overlapping walls. These walls enabled the rinsing of excess photoresist after the exposure process and provided free access of the test substance to the FP resonator cavity during measurement.

The considered structures are printed directly on the end-face of the optical fibers using the Photonic Professional 3D femtosecond direct laser writing system, Nanoscribe Professional GT2. For printing photoresist IP-Dip2 from Nanoscribe (with a refractive index of 1.52 @1550 nm after polymerization) was used [17]. The structures of the tips were designed in CAD software and printed to ensure the smoothest possible surfaces for the mirrors [18]. To enhance adhesion between the fiber and printed structures, laser direct writing begins a few nanometers inside the fiber, but not too deep to avoid heating the surface or the photoresin.

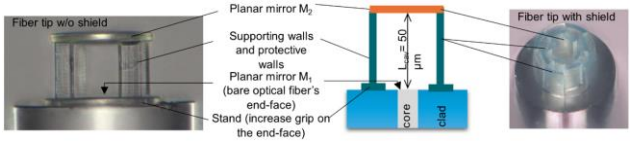

Fig. 1. Scheme and photos of the obtained 3D printed fiber tip in two configurations: unshielded (left) and shielded (right).

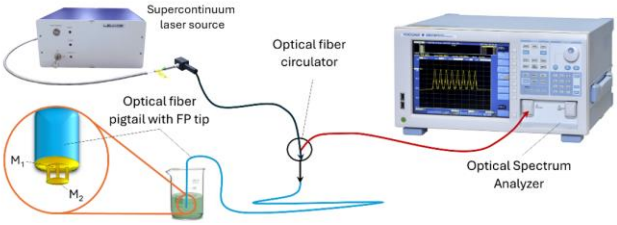

Fig. 2. Measurement setup.

The measurement setup is shown in Fig. 2. The signal from the supercontinuum laser source (Leukos, MIR 4.1) was transmitted to an optical circulator, which in turn directed it to the fiber optic tip. After reflecting from the FP resonator, it returned to the circulator and was measured using a YOKOGAWA AQ6370C Optical Spectrum Analyzer (OSA) covering 600–1700nm with a resolution of 0.1nm. The broadband source used in the experiment enabled testing of the proposed solution across a wide range of fiber optic networks, from the O band to the U band. Finally, printed FP resonators were tested in benzene alcohol and isopropanol (IPA), with refractive indices of 1.477 and 1.374 at 1550nm, respectively, to verify whether the sputtered mirrors enable expanding the range of application of the designed tip. Sensitivity measurements were performed for propanol-toluene mixtures, allowing for a change in the refractive index in the range between 1.376 and 1.478 with a step of 0.01 RIU.

First, we tested how the printed FP resonator would perform without any gold layer sputtered onto it. The measurements were performed at room temperature and atmospheric pressure. As shown in Fig. 3, when the tip

was measured before immersion, a three-wave resonance was observed, resulting in a Vernier effect in the reflected spectrum. Based on analysis of the observed signal, we can calculate that the FSR is 21.6nm, which corresponds to the modelled L_{cav} (Table 1). Additionally, we can observe a Vernier effect envelope of 163nm in the signal, which corresponds to the 5μm thickness of the flat reflective surface.

After immersing the FP resonator in IPA, the quality of the reflected signal decreased significantly. The resonance spectrum is only visible at wavelengths most strongly emitted by the supercontinuum laser source (1450–1650 nm). After immersing the FP resonator in benzene alcohol, the signal completely disappeared. The only noticeable signal is a small signal resulting from the reflection of the most characteristic wavelength, 1550 nm, from the pump of the supercontinuum laser source. It follows that the very low refractive index contrast between polymerized IP-Dip2 and benzene alcohol requires high light intensity to be noticed in the reflected spectrum, which is not a desirable effect.

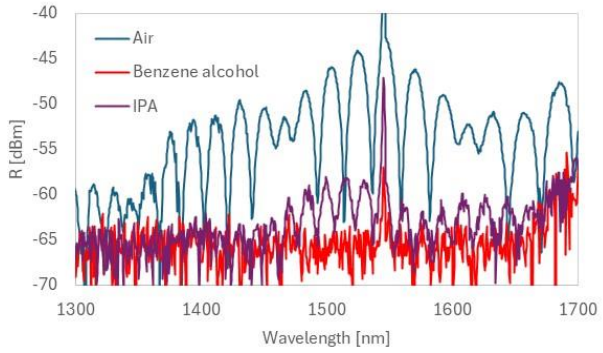

Fig. 3. Spectral analysis for an unshielded tip with different materials filling the FP resonators.

The solution to this problem is to sputter a metal layer onto the reflective surfaces in the FP resonator. It should be noted that the gold layer was sputtered onto the upper surface of the flat reflective surface and onto the optical fiber surface. The lower surface of the flat reflective surface was not sputtered, reducing its significance in the reflected spectrum. Therefore, the Vernier effect is no longer visible in the subsequent results.

As presented in our previous work [9], the best results are obtained when the difference in sputtering thickness between the two mirrors is significant. We got the improved result when mirror M_1 was sputtered with a 5nm layer of gold. Further increasing the sputtering thickness of mirror M_1, first to 12nm and then to 30nm, reduces the extinction ratio to 3dB and then to zero, respectively. This is because after the initial improvement in the ratio of the reflected signals from the individual mirrors observed for a small sputtering thickness on mirror M_1, further increasing this thickness reduces the amount of light reaching mirror M_2.

During the sputtering process, the upper mirror (M_2) will always be coated with a thicker layer than the lower mirror (M_1). This is because the gold sputtering technology used in the experiment is unidirectional. However, a small fraction of the gold particles will always fall onto mirror M_1, creating a reflective layer that is disproportionately thinner than the layer formed on mirror M_2 (Fig. 4). To better control the differences in the sputtering degree of both mirrors, we attempted to obscure mirror M_1. This can be achieved by selecting the width of the supports supporting mirror M_2 at the appropriate height.

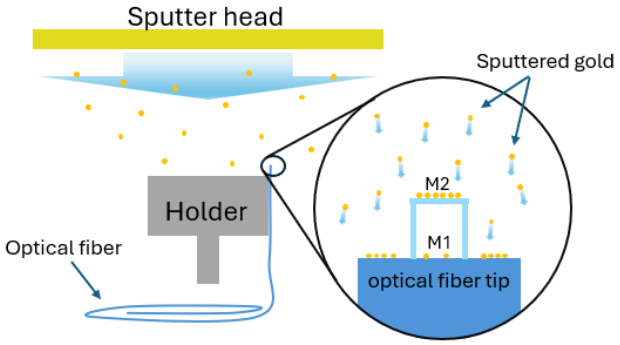

Fig. 4. Schematic diagram of sputtering a gold layer onto a fiber optic tip.

We performed spectral analysis on shielded and unshielded tips sputtered with a 10 nm gold layer each. As shown in Fig. 5, the unshielded tip exhibits a higher extinction ratio than the shielded tip. This is due to the fact that a small layer of gold covered the M_1 mirror in the unshielded tip, which improved the ratio of the reflected light intensities between the two mirrors. In the case of the shielded tip, the M_1 mirror was effectively shielded by the set of supports, and no gold layer appeared on it.

Filling both FP resonators with a material with a similar refractive index (benzene alcohol) to the photopolymer used to print the tips (IP-Dip2) further highlighted the advantages of the sputtered mirror solution (Fig. 6). The shielded tip with the unsputtered M_1 mirror is characterized by a very low extinction ratio (2.2dBm). The unshielded tip, however, significantly increased its extinction ratio up to 15.2dBm. This value enables the use of a sensor based on an FP resonator, even when the refractive index of the measured material and the measuring head are identical. Additionally, as shown in Fig. 5, the unshielded tip enables measurements with similar accuracy across a wide wavelength range, from 1350nm to 1700nm. Additionally, it can be seen that the signal modulation level of the unshielded tip increased from 12.2dBm to 15.2dBm during immersion in benzene

alcohol (Fig. 6), compared to the level observed before immersion (Fig. 5).

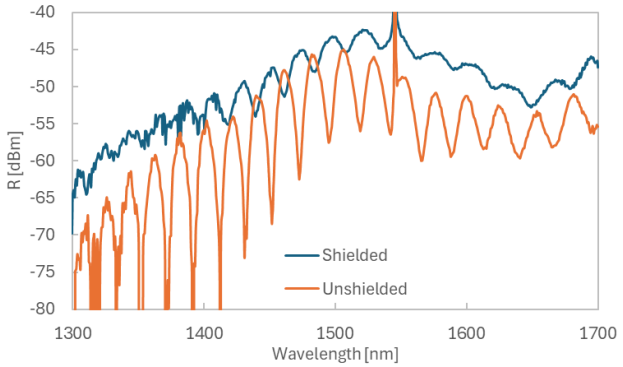

Fig. 5. Spectral analysis for shielded and unshielded tips in air.

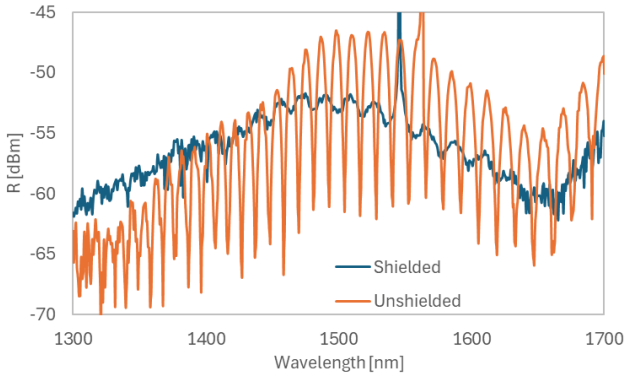

Fig. 6. Spectral analysis for shielded and unshielded tips immersed in benzene alcohol.

The data presented in Table I, obtained for both FP resonators before and after filling with benzene alcohol, show that the experimental results agree with those calculated based on the catalogue data. As expected, the FSR decreased after filling the FP resonator with benzene alcohol. Table II shows that the FP resonator parameters, such as Q-factor and Finesse (F), are comparable to those observed in the literature. However, it should be noted that the systems presented in [11] or [12] are much more complex.

We then checked whether the sensitivity of this sensor would change after sputtering the mirrors with a few-nanometer-thick gold layer. The measurement setup presented in Fig. 2 was used to test the Fabry-Pérot fiber optic sensor. In Fabry-Pérot resonators, the change in RIU of the cavity-filling material is equal to the change in wavelength. The relative change in RIU can be calculated using the following equation [19]:

$$\Delta n = \frac{\Delta\lambda}{\lambda} n \tag{5}$$

where n is the initial RIU of the measurement media in the microcavity, λ is the initial wavelength corresponding to any of the interference minima, and Δλ is the change in λ when n changes by Δn.

TABLE I
Comparison of the FRS value calculated from Eq. (4) and measured in the experiment

MATERIALS	AIR	BENZENE
L_{cav}	50 µm	50 µm
λ	1500 nm	1500 nm
n [@1500nm]	1.0	1.477
FSR [calculated]	20.5 nm	13.8 nm
FSR [unshielded]	21.6 nm	14.8 nm
FSR [shielded]	27.2 nm	16.0 nm

TABLE II
Comparison of the measured Q-factor and Finesse with literature data

	MEASURED	LITERATURE
L_{cav}	50 µm	50 µm
λ	1550 nm	1550 nm
n [@1500nm]	1.377	1.377
Q-factor	478 ± 5	530 ± 8 [11] 224 ± 12 [12]
Finesse	4.43 ± 0.05	–

Sensitivity measurements were performed for propanol-toluene mixtures, allowing for a change in the refractive index in the range between 1.376 and 1.477. The RI variation range was chosen to demonstrate the limits of applicability of the Fabry-Pérot fiber optic sensor without sputtered mirrors. At the same time, we aimed to verify the linearity of the sensor variations to the greatest extent possible and compare the results with the theoretical predictions described by Eq. (5). Considering that the FSR is 11µm for a wavelength of 1300nm and an RI of 1.4, the RI varied by 0.005. This RI variation enables a shift of the resonance peak by 4.5µm, which falls within the FSR. Unfortunately, in some cases, a small deviation in the obtained RI value resulted in an increase in Δλ [from Eq. (5)] above the FSR, as you can see in Fig. 7.

Figure 8 compares the sensitivity of both sensor types (with sputtered and unsputtered mirrors) with the sensitivity described by Eq. (5). As can be seen in the graph, sputtering the mirrors does not affect the sensitivity of the Fabry-Pérot fiber optic sensor, which is 930nm/RIU at a wavelength of 1300nm. This value is consistent with the sensitivity calculated using Eq. (5), which is represented by the black line in Fig. 8. Simultaneously, Fig. 8 shows the limit of applicability of

the Fabry-Pérot fiber optic sensor without sputtered mirrors (orange squares).

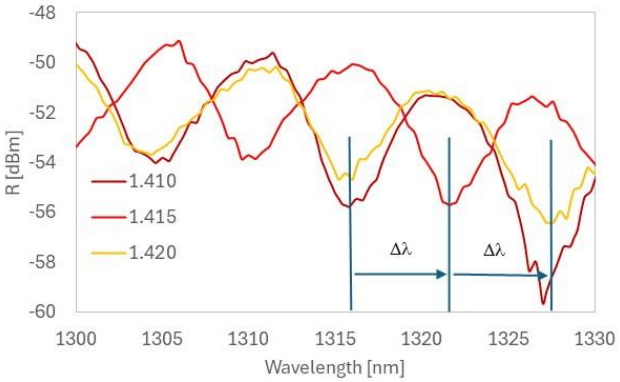

Fig. 7. Spectral analysis of the Fabry-Pérot fiber optic sensor without sputtered mirrors.

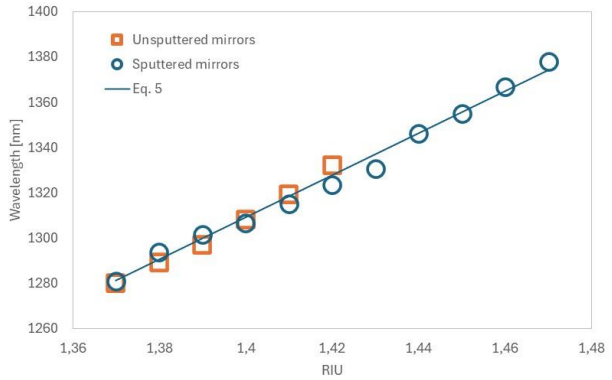

Fig. 8. Comparison between the sensitivities of the Fabry-Pérot fiber optic sensors (with sputtered and unsputtered mirrors) and the theoretical sensitivity.

This study demonstrated the feasibility of constructing a very simple 3D-printed fiber optic tip with an FP resonator, enabling the measurement of refractive index over a very wide range. This measurement specifically covers the refractive index range around 1.55. This was achieved by additionally depositing gold layers on the mirrors of the FP resonator. These layers were deposited using a simple sputtering device designed for depositing metallic surfaces. By using unidirectional sputtering, a corresponding difference in the gold layers on the individual mirrors was achieved. Mirror M_1 has a much lower reflectance than mirror M_2. This allows the FP resonator to measure the change in the refractive index of the tested liquid regardless of the material from which the resonator is made.

The research was funded by Warsaw University of Technology within the Excellence Initiative: Research University (IDUB) program and partially by the National Science Centre, Poland, under research project no. UMO-2020/39/B/ST7/02356.

References

[1] X. Zhang, L. Shao, X. Zou, B. Luo, W. Pan, and L. Yan, Opt. Lett. **42**(17), 3474 (2017).
[2] C. Massaroni, P. Saccomandi, E. Schena, J. Funct. Biomat. **6**(2), 204 (2015).
[3] G. Berruti, M. Consales, M. Giordano, L. Sansone *et al*. Sensors Actuators B: Chemical **77**, 94 (2013).
[4] S.J. Mihailov, Sensors **12**(2), 1898 (2012).
[5] Y. Chen *et al*., Sensors **22**(15), 5748 (2022).
[6] H. Wei, M. Chen, S. Krishnaswamy, Appl. Opt. **59**(7), 2173 (2020).
[7] Y. Shang, Q. Ni , D. Ding, N. Chen, T. Wang , Optoelectr. Lett. **11**(1), 61 (2015).
[8] Osório, J.H., Rodrigues, G.L., Morais *et al*., Discov. Sens. **1**, 2 (2025).
[9] J. Korec-Kosturek, M.M. Halendy, S. Ertman, P. Lesiak, Proc. SPIE **130010**, 130010L (2024).
[10] M.M. Halendy, J. Korec-Kosturek, S. Ertman, P. Lesiak, T. Woliński, Proc. SPIE **130010**, 130010M (2024).
[11] J.C. Williams, H. Chandrahalim, J.S. Suelzer, N.G. Usechak, Adv. Phot. Res. **3**(7), 2100359 (2022).
[12] J.C. Williams, H. Chandrahalim, J.S. Suelzer, N.G. Usechak, ACS Appl. Mater. Interfac. **14**(17), 19988 (2022).
[13] N. Sathitanon, S. Pullteap, PEWASET **26**, 526 (2007).
[14] M. Suter, P. Dietiker, Appl. Opt. **53**(30), 7004 (2014).
[15] L. Chen, Q. Wu, Scient. Rep. **15**, 6419 (2025).
[16] Y. Zhao, C. Li, Z. Lin, Y. Wang, R. Tong, L. Cai, Sensors Actuators B: Chemical **416**, 135999 (2024).
[17] Y. Li, S. Park, M. McLamb, M. Lata, S. Schöche, D. Childers, I.D. Aggarwal, M.K. Poutous, G. Boreman, T. Hofmann, Opt. Mater. Expr. **9**, 4318 (2019).
[18] A.K. Varshneya, Sheffield: Society of Glass Technology **1**, 477 (2013).
[19] I. M. White, X. Fan, Opt. Expr. **16**, 1021 (2008).